The following article appeared in *IFAC-PapersOnLine 51(13): 526-531 (2018);* and may be found at: https://doi.org/10.1016/j.ifacol.2018.07.333

Available online at www.sciencedirect.com

ScienceDirect

IFAC PapersOnLine 51-13 (2018) 526–531

Analysis of a Class of Complex System without Equilibria via Switched Control Law

R.J. Ecalante-González* E. Campos-Cantón**

División de Matemáticas Aplicadas,
Instituto Potosino de Investigación Científica y Tecnológica A.C.
Camino a la Presa San José 2055 Col. Lomas 4a Sección, 78216,
San Luis Potosí, S.L.P., México
**e-mail: rodolfo.escalante@ipicyt.edu.mx*
***e-mail: eric.campos@ipicyt.edu.mx*

Abstract:
In this article we introduce a new class of complex system without equilibria which exhibits a chaotic multiscroll attractor in each node. The number of scrolls in the attractor is determined by a switched control law to allow the operation of different linear affine systems. Thus, the system is composed of many subsystems which interact with each other to generate a multiscroll attractor. This new class of piecewise linear (PWL) system presents no positive real part in the eigenvalues of the Jacobian matrix as opposed to the reported systems with multiscrolls. The scrolls present a complex behavior since these don't unwrap and don't appear close to an unstable manifold of a saddle-focus equilibrium point. A particular case is taken as case study and simulation plots of the attractor are provided.

Keywords: Chaos theory, chaotic behaviour, piecewise linear controllers, piecewise linear systems, systems without equilibria

1. INTRODUCTION

The study of dynamical systems without equilibria has attracted the attention of the scientific community in recent years. One of the first dynamical systems presenting oscillations and no equilibria was described by Arnold Sommerfeld in 1902 (Kiseleva et al. (2016)). However the first system without equilibria with a chaotic flow was reported by Sprott in 1994 (Sprott (1994)) and was called Sprott case A. The associated vector field of this system presents two quadratic nonlinearities and is a particular case of the Nose-Hoover system (Hoover (1995)).

The attractors exhibited by these systems without equilibria fall into the category of hidden attractors according to the definition given by Leonov et al. (2011), since the basin of attraction does not intersect with small neighborhoods of equilibria. There are also more recent three-dimensional dynamical systems without equilibria reported with quadratic nonlinearities in its description, as the one in Wei (2011) which is based on the Sprott case D system or the seventeen flows found by three numerical methods proposed in Jafari et al. (2013). The previous works have reported three-dimensional complex systems, but higher dimentions have also been explored, for example, four-dimensional chaotic and hyperchaotic dynamical systems without equilibria through the use of quadratic and/or cubic nonlinearities have also been reported in Wang et al. (2012), Pham et al. (2016), Tahir et al. (2015). PWL dynamical systems are known to be capable of producing chaos, an example of this is the well studied Chua system. Furthermore hyperchaotic piecewise linear systems without equilibria have been reported, as the four-dimensional hyperchaotic system introduced in Li et al. (2014). This system was obtained from an approximation made to an extended system based on the diffusionless Lorenz system. On the other hand, there is a class of systems that show complex dynamics different from the multiscroll attractors, instead, they display multiwing attractors. For example, a four-dimensional chaotic systems capable of producing a multiwing butterfly chaotic attractor was presented in Tahir et al. (2015).

Recently, new approaches to get chaotic attractor in systems without equilibria based on piecewise linear systems were introduced in Escalante-González and Campos-Cantón (2017) and Escalante-González et al. (2017). In the same spirit that the aforementioned works, in this paper a new class of piecewise linear (PWL) system without equilibria is reported. The new class is interesting since these systems present a multiscroll attractor whose scrolls don't unwrap close to an unstable manifold of an equilibrium point as the current reported systems. Moreover the switched control law ensures the absence of equilibrium points and determine the number of scrolls exhibited by the attractor.

It is well known that no system without equilibria has a linear associated vector field of the form $\dot{x} = Ax$, in order to have a system without equilibria the vector field

Peer review under responsibility of International Federation of Automatic Control.
10.1016/j.ifacol.2018.07.333

should be at least linear affine of the form $\dot{x} = Ax + B$, however, a correct vector B should be chosen and the absence of equilibria does not imply a bounded flow in a region of the state space. Thus, to get a chaotic attractor in a system without equilibria is necessary to consider a PWL vector fields. This can be achived by considering a switched control law that is applied to generate a set of linear affine systems.

In section 2 basic theory of PWL systems and switched control laws is given. In section 3 a possible electronic realization for a chaotic attractor in a system without equilibria with one scroll is introduced. In section 4 a new class of dynamical systems without equilibria with multiscroll attractors is presented along with a particular case and its electronic realization. In section 5 a new class of complex system without equilibria with a multiscroll attractor in each node is presented.

2. PIECEWISE LINEAR SYSTEMS

A dynamical system is said to be a piecewise linear if it has an associated vector field of the form

$$\dot{x} = f(x) = \begin{cases} A_1x + B_1, & \text{if} \quad x \in D_1; \\ A_2x + B_2, & \text{if} \quad x \in D_2; \\ \quad\vdots & \quad\vdots \qquad \vdots \\ A_nx + B_m, & \text{if} \quad x \in D_m; \end{cases} \tag{1}$$

where B_i could be zero, D_i with $i = 1, 2, \ldots, m$ are the domains of each sub-system, and $\bigcup_{i=1}^{m} D_i = \mathbb{R}^n$ y $\bigcap_{i=1}^{m} D_i = \emptyset$.

The vector field defined by $f : \mathbb{R}^n \to \mathbb{R}^n$, for a PWL system without equilibria, should satisfy certain requirements in order to avoid equilibria of the system.There are two approaches to get this. The former is by considering that linear operators A_i are not singular, so each domain D_i, assigned to a linear or linear affine transformation $A_ix + B_i$, must not contain an equilibrium point given by $x^* = -A^{-1}B_i$, *i.e.*, there is not equilibrium point due to $x^* \notin D_i$, instead, $-A_i^{-1}B_i \in D_j$ with $i \neq j$. The second approach is given by considering that linear operators A_i are singular, so the linear affine vector field $\dot{x} = A_ix + B_i$ has no equilibria in all $\mathbb{R}^n$. In this work we consider the last approach.

Without loss of generality, we will assume the same A matrix for all domains D_i, with $i = 1, \ldots, n$. Therefore, the system (1) can be rewritten as follows:

$$\dot{x} = Ax + B(x), \tag{2}$$

where $B(x)$ is handled by the switched control law.

3. SYSTEM WITH ONE SCROLL

Definition 1. (UDSWE). A dynamical system with an associated vector field of the form $f(x) = Ax + B$ is an Unbounded Dissipative System Without Equilibria (UDSWE) if $A = [a_1,\ a_2,\ a_3] \in \mathbb{R}^{3\times3}$ whose characteristic polynomial $P_A(\lambda)$ has the roots $\{\lambda_{1,2} = p \pm iq,\ \ \lambda_3 = 0\}$ with $p < 0$, $q \neq 0$ and B is a linear combination of the form

$$B = k_1a_1 + k_2a_2 + k_3a_3 + k_4v,$$

where $k_4 \neq 0$ and v fulfills $Av = 0$ and $v \neq 0$.

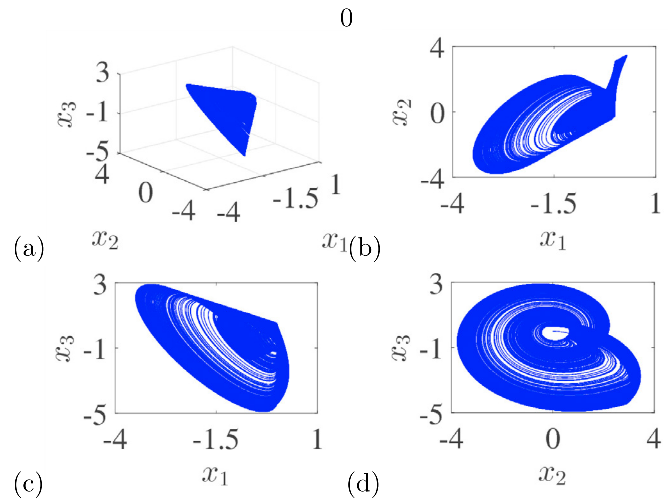

Fig. 1. Attractor of the system (2) with the switched control law (3) with A, B_1 and B_2 given in (4) for the initial condition $x_0 = (0,\ 0,\ 0)^T$ in the space (a)$x_1 - x_2 - x_3$ and its projections onto the planes: (b) $x_1 - x_2$, (c) $x_1 - x_3$ and (d) $x_2 - x_3$.

Consider the dynamical system introduced in Escalante-González and Campos-Cantón (2017) given by (2) with the switched control law:

$$B(x) = \begin{cases} B_1, \text{ if } x_1 < \sigma; \\ B_2, \text{ if } x_1 \geq \sigma. \end{cases} \tag{3}$$

and:

$$A = \begin{bmatrix} 0 & 1 & 1 \\ 0 & -0.5 & 3 \\ 0 & -3 & -0.5 \end{bmatrix}, B_1 = \begin{bmatrix} 0.5 \\ 0 \\ 0 \end{bmatrix}, B_2 = \begin{bmatrix} -1 \\ 10 \\ 0 \end{bmatrix}. \tag{4}$$

In this case $\dot{x} = Ax + B_1$ and $\dot{x} = Ax + B_2$ are UDSWE systems and have no equilibria in all $\mathbb{R}^3$. This system generates a chaotic attractor located around the plane $x_1 = \sigma$. The resulting attractor for $\sigma = 0$ is shown in Figure 1.

3.1 Electronic realization

In this subsection a possible electronic realization for the system (2) with the switched control law (3) with A, B_1 and B_2 given in (4) is presented. The electronic circuit is designed to be energized by DC power sources of ±12V and ±15V and is shown in Figure 2. The circuit diagram has been divided in five sub-diagrams.

The sub-circuits in the sub-diagrams in Figures 2a and 2b consist of an operational amplifier (op amp) configured as adder-subtractor followed by an op amp configured as an integrator, these are the responsible circuits for the signals x_1 and x_2, respectively.

The sub-diagram in Figure 2c consists of an op amp configured as an adder followed by an op amp configured as an integrator and its designed to produce the signal x_3.

The gains of the adder in the sub-circuit of x_3 were chosen according to the third row vector of the matrix A, while the gains of the adder-subtractor of the sub-circuits of x_1 and x_2 were designed according to the first two row vectors of the matrix A and considering an additional gain of -1 reserved for signals A and B, respectively.

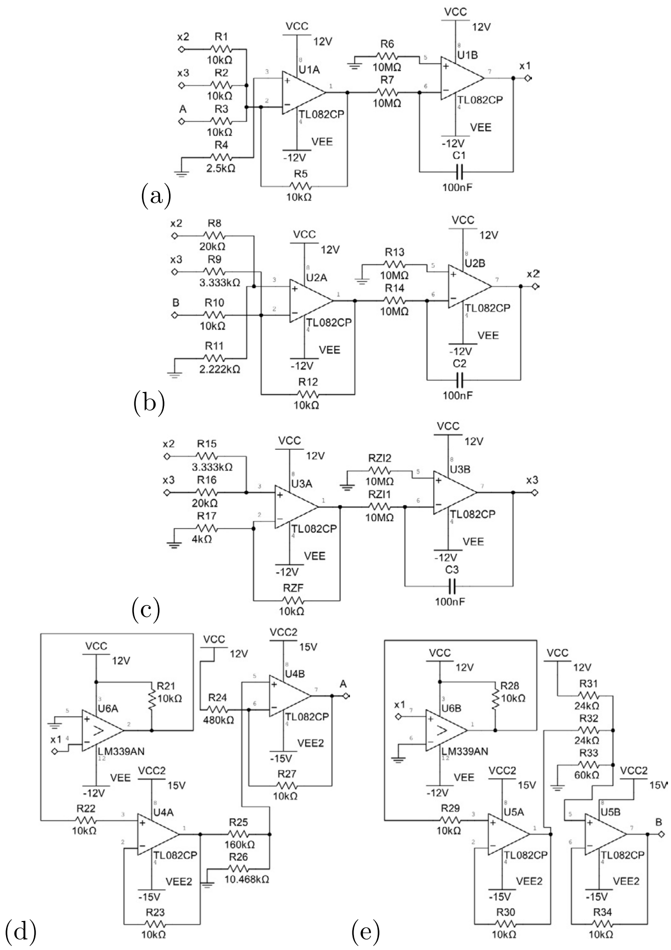

Fig. 2. Sub-diagrams of the proposed electronic realization of the system (3) with A, B_1 and B_2 given in (4) for the sub-circuits that produce the output signals: (a) x_1 (b) x_2, (c) x_3, (d) A and (e) B.

The sub-circuits in the sub-diagrams of Figures 2d and 2e consist of a comparator followed by an op amp configured as a buffer and an adder in the first case and an adder-subtractor in the second one. These two sub-circuits are responsible for the commutation of B_1 and B_2.

The electronic circuit makes use of the general purpose JFET-input dual Operational amplifier TL082CP and the quad differential comparator LM339AN. Mathematical resistor values calculated were approximated to achievable values by one or two resistors from the E12 series combined either in parallel or series.

An electronic simulation of the proposed circuit has been run and the result is shown in Figure 3.

Furthermore, experimental results are shown in Figure 4.

4. MULTISCROLL SYSTEM

The term multiscroll attractor is used to refer to three or more scrolls in an attractor Campos-Cantón et al. (2010). In this section a system with a triple scroll is proposed.

Consider a system

$$\dot{x} = Ax + B(x, \sigma(x)), \tag{5}$$

with A given as follows:

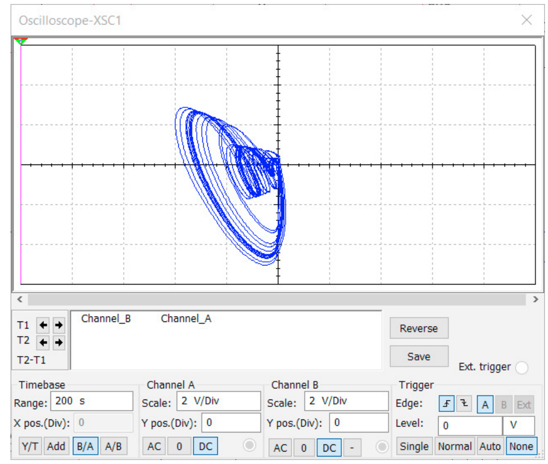

Fig. 3. Attractor of the circuit diagram in Figure 2 generated by electronic simulation projected on the plane $x_1 - x_3$.

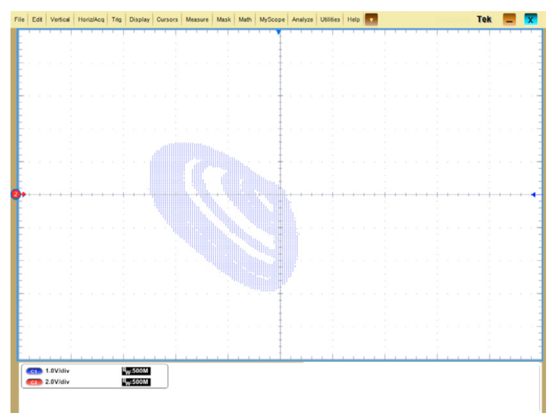

Fig. 4. Attractor of the circuit diagram in Figure 2 projected onto the plane $x_1 - x_3$ obtained experimentally.

$$A = \begin{bmatrix} 0 & 0 & 0 \\ 0 & -a & b \\ 0 & -b & -a \end{bmatrix}. \tag{6}$$

where $a, b \in \mathbb{R}_{>0}$, i.e. the roots of $P_A(\lambda)$ are $\lambda_{1,2} = -a \pm ib$ and $\lambda_3 = 0$.

For the switched control law, five commutation planes are considered:

$$\begin{aligned} S_{u_1} &= \{x \in \mathbb{R}^3 | \gamma_1 x_1 + \gamma_2 x_2 + \gamma_3 x_3 = \gamma_3(\epsilon_1 + \epsilon_2)\}, \\ S &= \{x \in \mathbb{R}^3 | \gamma_1 x_1 + \gamma_2 x_2 + \gamma_3 x_3 = 0\}, \\ S_{d_1} &= \{x \in \mathbb{R}^3 | \gamma_1 x_1 + \gamma_2 x_2 + \gamma_3 x_3 = -\gamma_3(\epsilon_1 + \epsilon_2)\}, \end{aligned} \tag{7}$$

with $\gamma_1 = 0.9027$, $\gamma_2 = 0.2441$, $\gamma_3 = -0.3543$ and

$$\begin{aligned} S_{\sigma_1} &= \{x \in \mathbb{R}^3 | x_3 = -\epsilon_2\}, \\ S_{\sigma_2} &= \{x \in \mathbb{R}^3 | x_3 = \epsilon_1\}, \end{aligned} \tag{8}$$

with $\epsilon_1, \epsilon_2 \in \mathbb{R}_{>0}$.

To write the switching control, law the notation $x > S$ will be used if x is in the set pointed by the vector $(\gamma_1,\ \gamma_2,\ \gamma_3)^T$, $x \leq S$ if x is in the opposite set or on the plane S.

The notation $x > S_{\sigma i}$ will be used if x is in the set pointed by the vector $(0,\ 0,\ 1)^T$, $x \leq S_{\sigma i}$ if x is in the opposite set or on the plane $S_{\sigma i}$.

The switched control law is then given by:

$$\sigma(x) = \begin{cases} -1, & \text{if} \quad x \leq S_{\sigma_1}; \\ 0, & \text{if} \quad S_{\sigma_1} < x \leq S_{\sigma_2}; \\ 1, & \text{if} \quad x > S_{\sigma_2}; \end{cases} \tag{9}$$

$$u = \begin{bmatrix} 0 \\ 0 \\ \sigma(x)(\epsilon_1 + \epsilon_2) \end{bmatrix}. \tag{10}$$

$$B(x, \sigma(x)) = \begin{cases} B_1 - \sigma(x)(\epsilon_1 + \epsilon_2)a_3, & \text{if} \quad x - u \leq S; \\ B_2 - \sigma(x)(\epsilon_1 + \epsilon_2)a_3, & \text{if} \quad x - u > S; \end{cases} \tag{11}$$

where

$$B_1 = \begin{bmatrix} b_{11} \\ b_{12} \\ b_{13} \end{bmatrix}, \; B_2 = \begin{bmatrix} b_{21} \\ b_{22} \\ b_{23} \end{bmatrix}, \tag{12}$$

such that $B_1, B_2 \in \mathbb{R}^3$ with $b_{11} > 0$, $b_{21} < 0$ and $b_{22}, b_{23} \neq 0$.

With an appropriate selection of parameters the system (5) exhibit a triple-scroll attractor.

Since the null space of A is $\text{null}(A) = \text{span}\{(1, \; 0, \; 0)^T\}$, A and $B(x, \sigma(x))$ fulfill the definition 1 for all x.

It is worth notice that the number of scrolls can be easily increased just by extending $\sigma(x)$ from -1 and 1 to $-n$ and m to have $m + n + 1$ number of scrolls.

Consider now the particular case with B_1 and B_2 as follows:

$$B_1 = \begin{bmatrix} 0.5 \\ 0 \\ 0 \end{bmatrix}, B_2 = \begin{bmatrix} -3.5128 \\ 9.4093 \\ 0.3543 \end{bmatrix}, \tag{13}$$

and the parameters given in Table 1.

Table 1. Parameters for a particular case

Parameter	Value
a	0.5
b	3
ϵ_1	2.6
ϵ_2	4.5

The resulting attractor is shown in Figure 5.

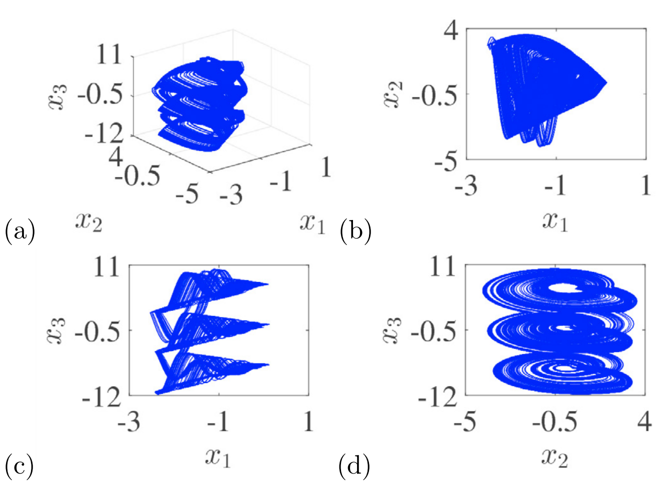

Fig. 5. Attractor of the system (5) with A given in (6) and the switching law given in (11) for the initial condition $x_0 = (0, \; 0, \; 0)^T$ in the space (a)$x_1 - x_2 - x_3$ and its projections onto the planes: (b) $x_1 - x_2$, (c) $x_1 - x_3$ and (d) $x_2 - x_3$.

The maximum Lyapunov exponent was calculated to be $MLE = 0.233936$ which is an indication of chaos.

4.1 Electronic realization

In this subsection a possible electronic realization for the system (5) with A given in (6) with the switching law given in (11) is presented. The electronic circuit is designed to be energized by DC power sources of ±12V and ±15V. The circuit diagram has been divided in eight sub-diagrams shown in Figures 6, 7 and 8.

The sub-circuit in the sub-diagram shown in Figure 6a consist of an op amp configured as an inverter followed by an op amp configured as integrator and it is responsible for the signal x_1.

The sub-circuits in the sub-diagrams shown in Figures 6b and 6c consist of a an op amp configured as adder-subtractor followed by an op amp configured as an integrator and are responsible for the signals x_2 and x_3.

The sub-diagrams in Figures 7a, 7b and 7c consist of a comparator followed by an op amp configured as buffer and another one either as adder-subtractor or adder. These sub-circuits are responsible for the signals A, B, and C, which together produce the change of the affine part based on the signal E coming from the adder-subtractor shown in Figure 8b. This sub-circuit depends on the signal D of the sub-circuit in Figure 8a which is composed of two comparators followed by op amps configured as buffers and an op amp configured as an adder.

This electronic circuit also makes use of the TL082CP and LM339AN devices and as the first circuit realization presented, the mathematical resistor values calculated were approximated to achievable values by one or two resistors from the E12 series combined either in parallel or series.

An electronic simulation has been run and the result is presented in Figure 9.

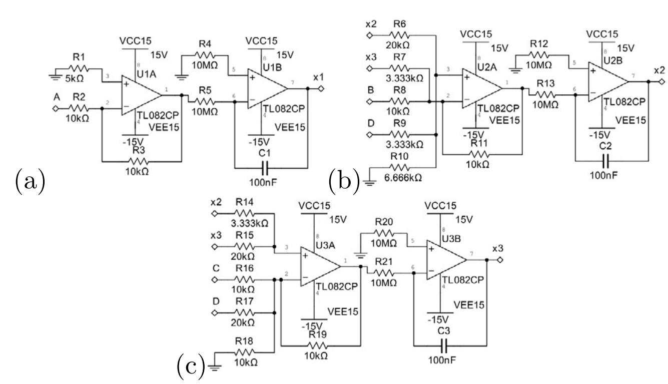

Fig. 6. Sub-diagrams of the proposed electronic realization of the system (5) with A given in (6) and the switching law given in (11) for the sub-circuits that produce the output signals: (a) x_1, (b) x_2 and (c) x_3.

5. COMPLEX SYSTEM WITHOUT EQUILIBRIA

In this section a new complex system without equilibria which exhibit a chaotic multiscroll attractor in each node

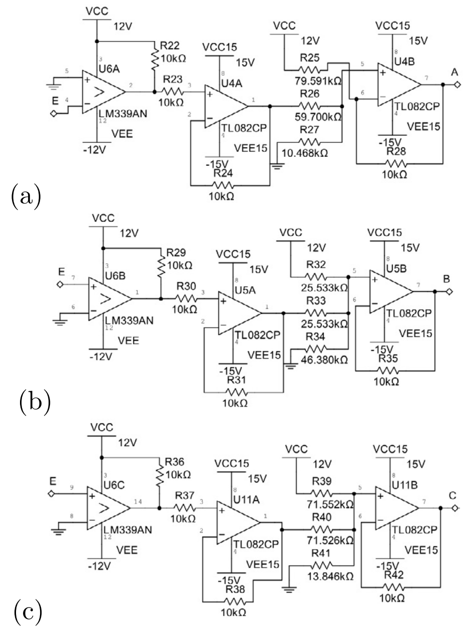

Fig. 7. Sub-diagrams of the proposed electronic realization of the system (5) with A given in (6) and the switching law given in (11) for the sub-circuits that produce the output signals: (a) A, (b) B and (c) C.

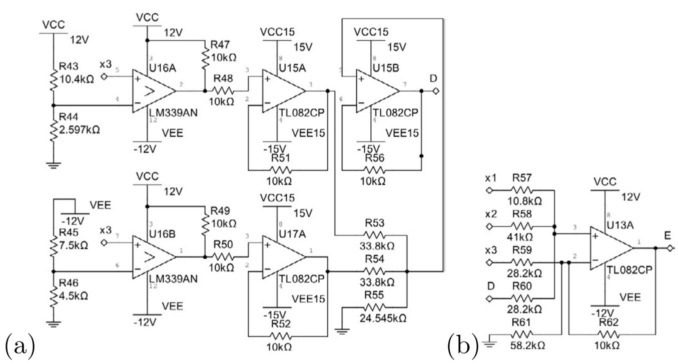

Fig. 8. Sub-diagrams of the proposed electronic realization of the system (5) with A given in (6) and the switching law given in (11) for the sub-circuits that produce the output signals: (a) D and (b) E.

is presented. The attractors synchronize due to a diffusive coupling between the identical systems (see Pecora et al. (1997)).

The description of any two identical nodes with dynamics $\dot{u} = F(u)$ and $\dot{v} = F(v)$ mutually coupled can be written as

$$\begin{aligned}\dot{u} &= F(u) + \alpha E(v-u);\\ \dot{v} &= F(v) + \alpha E(u-v).\end{aligned} \tag{14}$$

where E determines the linear combination of state components used in the difference and α is the coupling strength. In order to select appropriate values for the matrix E and α, the stability of the origin in the difference vector field $\dot{w} = \dot{u} - \dot{v}$ is studied. The system $\dot{w}$ can be expressed in Taylor expansion and approximated by neglecting higher order terms. In the case of systems of the form (2) the Jacobian matrix is equal to the matrix of the system. Thus, locally the stability could be studied in the system

$$\dot{w} \approx Aw - 2E\alpha w. \tag{15}$$

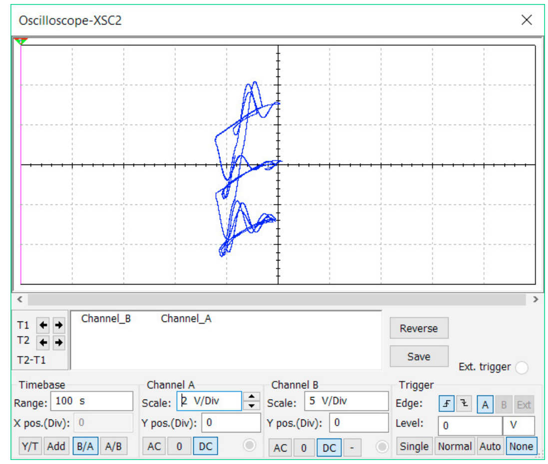

Fig. 9. Attractor of the circuit diagrams in Figures 6 and 7 generated by electronic simulation projected on the plane $x_1 - x_3$.

Consider the complex system given by a network where three nodes whose dynamic $\dot{x} = F(x)$, $\dot{y} = F(y)$ and $\dot{z} = F(z)$ are given by (5) with A given in (6) and the switching law given in (11) are connected with each node (see Figure 10). Each node exhibit a chaotic multiscroll attractor and the coupling used to synchronize the attractors is given as follows:

$$\begin{aligned}\dot{x} &= F(x) + \alpha_1 E_1(y-x) + \alpha_3 E_3(z-x);\\ \dot{y} &= F(y) + \alpha_1 E_1(x-y) + \alpha_2 E_2(z-y);\\ \dot{z} &= F(z) + \alpha_2 E_2(y-z) + \alpha_3 E_3(x-z);\end{aligned} \tag{16}$$

with $\alpha_1 = 0.5$ and $\alpha_2 = \alpha_3 = 3$ and where:

$$E_1 = \begin{bmatrix}1&0&0\\0&0&0\\0&0&0\end{bmatrix},\; E_2 = \begin{bmatrix}0&0&0\\0&1&0\\0&0&0\end{bmatrix},\; E_3 = \begin{bmatrix}1&0&0\\0&0&0\\0&0&1\end{bmatrix}. \tag{17}$$

Since the A matrix of the system has no eigenvalues with positive real part the coupling strengths could be restricted to $\alpha_1, \alpha_2, \alpha_3 \in \mathbb{R}_{>0}$.

In the Figure 11 comparisons in time of the corresponding states of each node are shown. The initial conditions were chosen so each node starts in a different scroll. As it can be seen from the plots, the synchronization take place at the beginning of the simulation starting at $t = 0$.

It is worth notice that the absence of equilibria guarantees the oscillation of the system in all the nodes for any initial condition in the basin of attraction.

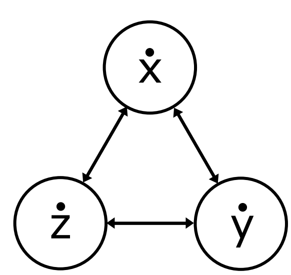

Fig. 10. Complex system with three identical nodes whose dynamical systems present a chaotic multiscroll attractor and no equilibria.

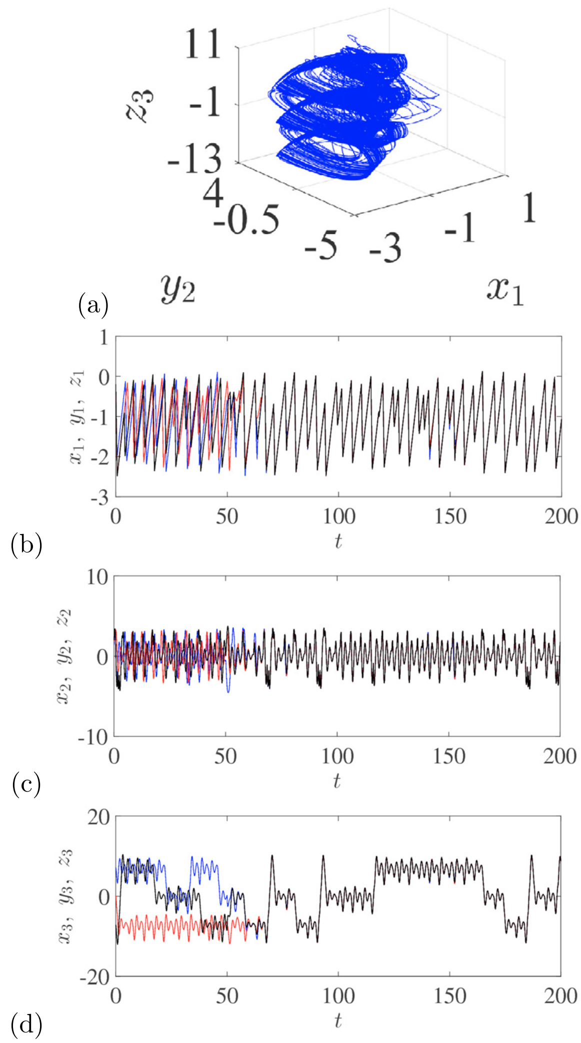

Fig. 11. Attractor generated by taking a state from each node of the complex system in the space (a)$x_1 - y_2 - z_3$. The comparison in time of the state variables (b)x_1, $y1$ and z_1, (c)x_2, y_2 and z_2 and (d)x_3, y_3 and z_3. The initial conditions where chosen as $x_0 = (-0.5,\ 1.5,\ 7.1)^T$, $y_0 = (-0.3,\ 1.8,\ 0.1)^T$ and $z_0 = (-0.2,\ 2,\ -7.1)^T$. The color for the plots in (b), (c) and (d) are blue, red and black for x, y and z, respectively.

6. CONCLUSION

In this paper a new class of complex system without equilibria which exhibits a chaotic multiscroll attractor in each node has been reported. The attractors of these systems differ from the current reported ones in the behavior and location of the scrolls. The differences in the behavior of the multiscroll attractors could lead to new ways to model physical phenomena. The absence of equilibrium points and the possibility of increasing the scroll number present a new way to design pseudo random number generators. These systems could be further studied for applications in secure communication, where absence of equilibria could be possibly used to increase the security.

ACKNOWLEDGEMENTS

R.J. Escalante-González Ph.D. student of control and dynamical systems at IPICYT thanks CONACYT for the scolarship granted (Register number 337188).

REFERENCES

Campos-Cantón, E., Barajas-Ramirez, J., Solís-Perales, G., and Femat, R. (2010). Multiscroll attractors by switching systems. *Chaos*, 20(1), 013116–1–6.

Escalante-González, R.J. and Campos-Cantón, E. (2017). Generation of chaotic attractors without equilibria via piecewise linear systems. *International Journal of Modern Physics C*, 28(1), 1750008–1–11.

Escalante-González, R.J., Campos-Cantón, E., and Nicol, M. (2017). Generation of multi-scroll attractors without equilibria via piecewise linear systems. *Chaos*, 27(5), 053109–1–8.

Hoover, W.G. (1995). Remark on 'some simple chaotic rows'. *Physical Review E*, 51(1), 759–760.

Jafari, S., Sprott, J., and Golpayegani, S.M.R.H. (2013). Elementary quadratic chaotic flows with no equilibria. *Physics Letters A*, 377, 699–702.

Kiseleva, M.A., Kuznetsov, N.V., and Leonov, G.A. (2016). Hidden attractors in electromechanical systems with and without equilibria. 49(14), 51–55.

Leonov, G., Kuznetsov, N., and V.I., V. (2011). Localization of hidden Chua's attractors. *Physics Letters A*, 375(23), 2230–2233.

Li, C., Sprott, J.C., Thio, W., and Zhu, H. (2014). A new piecewise linear hyperchaotic circuit. *IEEE Transactions on Circuits and Systems—Part II: Express Briefs*, 61(12), 977–981.

Pecora, L.M., Carroll, T.L., Johnson, G.A., and Mar, D.J. (1997). Fundamentals of synchronization in chaotic systems, concepts, and applications. *Chaos*, 7(4), 519–543.

Pham, V.T., Vaidyanathan, S., Volos, C., Jafari, S., and Kingni, S.T. (2016). A no-equilibrium hyperchaotic system with a cubic nonlinear termviet. *Optik*, 127(1), 32593265.

Sprott, J. (1994). Some simple chaotic flows. *The American Physical Society, Physical Review E*, 50(2), 647–650.

Tahir, F.R., Jafari, S., Pham, V.T., Volos, C., and Wang, X. (2015). A novel no-equilibrium chaotic system with multiwing butterfly attractors. *International Journal of Bifurcation and Chaos*, 25(4), 1550056–1–11.

Wang, Z., Cang, S., Ochola, E.O., and Sun, Y. (2012). A hyperchaotic system without equilibrium. *Nonlinear Dynamics*, 69, 531–537.

Wei, Z. (2011). Dynamical behaviors of a chaotic system with no equilibria. *Physics Letters A*, 376, 102–108.